

The Papain-Like Protease of Severe Acute Respiratory Syndrome Coronavirus Has Deubiquitinating Activity

Naina Barretto,¹ Dalia Jukneliene,¹ Kiira Ratia,² Zhongbin Chen,^{1,3} Andrew D. Mesecar,²
and Susan C. Baker^{1*}

Department of Microbiology and Immunology, Loyola University Chicago, Stritch School of Medicine, Maywood, Illinois¹; Center for Pharmaceutical Biotechnology and Department of Medicinal Chemistry and Pharmacognosy, University of Illinois at Chicago, Chicago, Illinois²; and Department of Biochemistry and Molecular Biology, Beijing Institute of Radiation Medicine, Beijing, China³

Received 12 July 2005/Accepted 19 September 2005

Replication of the genomic RNA of severe acute respiratory syndrome coronavirus (SARS-CoV) is mediated by replicase polyproteins that are processed by two viral proteases, papain-like protease (PLpro) and 3C-like protease (3CLpro). Previously, we showed that SARS-CoV PLpro processes the replicase polyprotein at three conserved cleavage sites. Here, we report the identification and characterization of a 316-amino-acid catalytic core domain of PLpro that can efficiently cleave replicase substrates in *trans*-cleavage assays and peptide substrates in fluorescent resonance energy transfer-based protease assays. We performed bioinformatics analysis on 16 papain-like protease domains from nine different coronaviruses and identified a putative catalytic triad (Cys1651-His1812-Asp1826) and zinc-binding site. Mutagenesis studies revealed that Asp1826 and the four cysteine residues involved in zinc binding are essential for SARS-CoV PLpro activity. Molecular modeling of SARS-CoV PLpro suggested that this catalytic core may also have deubiquitinating activity. We tested this hypothesis by measuring the deubiquitinating activity of PLpro by two independent assays. SARS-CoV-PLpro hydrolyzed both diubiquitin and ubiquitin-7-amino-4-methylcoumarin (AMC) substrates, and hydrolysis of ubiquitin-AMC is approximately 180-fold more efficient than hydrolysis of a peptide substrate that mimics the PLpro replicase recognition sequence. To investigate the critical determinants recognized by PLpro, we performed site-directed mutagenesis on the P6 to P2' residues at each of the three PLpro cleavage sites. We found that PLpro recognizes the consensus cleavage sequence LXGG, which is also the consensus sequence recognized by cellular deubiquitinating enzymes. This similarity in the substrate recognition sites should be considered during the development of SARS-CoV PLpro inhibitors.

The SARS coronavirus (SARS-CoV) was discovered to be the etiologic agent of an outbreak of atypical pneumonia that emerged out of southern China in the fall of 2002 (reviewed in references 41, 42, and 50). During the outbreak, the mortality from SARS-CoV infection was approximately 10%, with mortality associated with the increased age of the patient and risk factors such as diabetes and heart disease (11). Epidemiologic studies indicated that SARS-CoV emerged from an animal reservoir, such as masked palm civets (15), and was subsequently passed person to person via respiratory droplets or contact with aerosolized virus or fomites (47, 57, 61). Rigorous public health measures were ultimately successful in controlling SARS outbreaks. However, reemergence of SARS-CoV from an animal reservoir is a potential risk for future epidemics. Therefore, current research efforts are focused on the rapid development of vaccines and therapeutics to prevent and treat SARS-CoV infection.

The coronaviruses are enveloped positive-strand RNA viruses that replicate in the cytoplasm of infected cells. Human coronaviruses such as 229E (HCoV-229E) and HCoV-OC43 (20) and the recently identified HCoV-NL63 (12, 55) and

HCoV-HKU1 viruses (58) are responsible for respiratory infections that range from common colds to pneumonia. Other animal coronaviruses such as avian infectious bronchitis virus (aIBV), porcine transmissible gastroenteritis virus (TGEV), and mouse hepatitis virus (MHV) cause respiratory, gastrointestinal, or neurologic disease (29). Coronaviruses have large RNA genomes (27 to 32 kb), and viral replication is mediated by the viral RNA-dependent, RNA polymerase, termed the replicase (reviewed in reference 63). The coronavirus replicase is initially translated from the 5'-most 21 kb of the 29.7-kb SARS-CoV genomic RNA to produce two replicase polyproteins, termed pp1a and pp1ab. These polyproteins are processed by replicase-encoded proteases, PLpro and 3CLpro, to generate 16 replicase products, termed nonstructural proteins (nsp) 1 to 16. The coronavirus replicase intermediates and processing products assemble on intracellular membranes to generate double-membrane vesicles (DMVs), which are the site of viral RNA synthesis (13, 14, 43).

Proteolytic processing of the coronavirus replicase polyprotein is essential for generating a functional replication complex (27). Therefore, the coronavirus replicase-encoded proteases, 3CLpro and PLpro, are potential targets for antiviral drug development. The chymotrypsin-like 3CLpro processes the replicase polyprotein at 11 sites, including cleaving itself from the polyprotein to generate a ~25-kDa protease product. Structural information and high-throughput screens using purified 3CLpro have led to the identification of candidate anti-

* Corresponding author. Mailing address: Department of Microbiology and Immunology, Loyola University Chicago, Stritch School of Medicine, 2160 South First Avenue, Bldg. 105, Maywood, IL 60153. Phone: (708) 216-6910. Fax: (708) 216-9574. E-mail: sbaker1@lumc.edu.

viral agents that inhibit SARS-CoV replication (2, 7, 59, 60). In contrast, no structural information is currently available for any coronavirus PLpro. Molecular modeling of a HCoV-229E papain-like protease suggested that a zinc-binding domain, which connects the left- and right-hand domains of a papain-like fold, might be important for protease activity and that protease activity is mediated by a cysteine-histidine catalytic dyad (19). Interestingly, many coronaviruses encode two functional papain-like proteases, termed PLP1 and PLP2 (or PL1pro and PL2pro). At least two coronaviruses, SARS-CoV and aIBV, encode only one functional papain-like protease, which we term PLpro. The coronavirus papain-like proteases have been shown to process the amino-terminal end of the replicase polyprotein to generate two or three replicase products (3, 4, 8, 17, 18, 25, 35), but the exact role of proteolytic processing in the viral replication cycle has not yet been elucidated.

For SARS-CoV, the PLpro domain is contained within nsp3, a 213-kDa membrane-associated replicase product. Previously, we cloned and expressed a 73-kDa SARS-CoV PLpro domain and developed a *trans*-cleavage assay to assess protease activity. We found that SARS-CoV PLpro can function in *trans* and that it is responsible for processing nsp1, nsp2, and nsp3 from the amino-terminal end of the replicase polyprotein (17). In addition, a recent report by Sulea and colleagues predicted that SARS-CoV PLpro may have deubiquitinating activity on the basis of shared structural features with a cellular deubiquitinating enzyme, herpesvirus-associated ubiquitin-specific protease (HAUSP) (21, 53). Furthermore, SARS-CoV PLpro was predicted to cleave the consensus sequence LXGG (54), which is also recognized by deubiquitinating enzymes. Sulea predicted that a "structural signature" in the substrate-binding pocket, which may be important for cleavage after the diglycine residues, is present in some, but not all, coronavirus papain-like proteases. Testing these intriguing predictions is critical for increasing our understanding of the role of proteases in coronavirus replication and for developing antiviral agents directed against this important target.

Here, we report the identification, purification, and characterization of a 316-amino-acid catalytic core domain of SARS-CoV PLpro that is soluble and highly active. Our studies provide experimental evidence supporting the hypothesis that PLpro requires a zinc-binding domain and a catalytic triad (Cys1651-His1812-Asp1826) instead of a catalytic dyad for protease activity. To measure the kinetics of protease and putative deubiquitinating activity, we purified a catalytic core of SARS-CoV PLpro and developed *in vitro* peptide hydrolysis and deubiquitinating assays. We found that purified PLpro hydrolyzed both diubiquitin and synthetic peptide substrates and that the ubiquitin substrate was hydrolyzed approximately 180-fold more efficiently than the peptide substrate. Finally, we show that SARS-CoV PLpro cleaves at the consensus cleavage site LXGG, which is also the target sequence recognized by many deubiquitinating enzymes.

MATERIALS AND METHODS

Cells. HeLa-MHV receptor cells were used for all transfection-based assays as previously described (25). The cells were maintained in Dulbecco's modified Eagle's medium (Invitrogen) with 10% fetal bovine serum, 2% penicillin-streptomycin, and 5 mM HEPES, pH 7.4.

Construction of SARS-CoV PLpro expression plasmids and site-directed mutagenesis. Regions of SARS-CoV PLpro were PCR amplified from parental plasmid pPLPro1541-2204 (17). The primer sequences are available on request. The PCR products were digested with the restriction enzymes EcoRI and BamHI, and the fragments were ligated into the corresponding sites of plasmid vector pcDNA3.1 V5His (Stratagene, La Jolla, Calif.). After transformation into *Escherichia coli* XL-1 Blue cells (Stratagene), bacteria were grown at 25°C.

Site-directed mutagenesis was performed to change specific residues in pPLPro1541-1855 or the substrate pNSP1-3* using synthetic oligonucleotides (sequences are available on request). QuikChange Mutagenesis (Stratagene) was performed according to the manufacturer's instructions, and sequence changes were confirmed by DNA sequencing.

For purposes of overexpressing and purifying protein, DNA regions encoding core domains of wild-type and mutant PLpro enzymes were PCR amplified and cloned into pET11a (Invitrogen) between the NheI and Bpu1102I sites. The final clones were verified by DNA sequencing and designated pET-SARS-CoV-PLpro1541-1855 wild type, C1651A, and D1826A.

Sequence comparison of coronavirus papain-like protease domains. The amino acid sequence of the single papain-like protease found in aIBV and paralogous papain-like protease domains 1 and 2 found in seven other coronaviruses were aligned using the program ALIGN (SciED) with the SARS-CoV PLpro catalytic core domain (amino acid sequences 1541 to 1855) as the reference sequence. The scoring matrix BLOSUM 62 was used to set the alignment parameters, and the similarity significance value cutoff was set at greater than or equal to 60%.

Purification of SARS-CoV PLpro. Three liters of *E. coli* BL21(DE3) cells, containing pET11a-SARS-CoV-PLpro1541-1855, were grown for 24 h at 25°C. Cells were pelleted by centrifugation and resuspended in 80 ml of buffer A (20 mM Tris, pH 7.5, 10 mM β -mercaptoethanol [BME]) containing 500 μ g of lysozyme. The cells were incubated for 10 min and then lysed via sonication using a 600-watt model VCX ultrasonicator. After the cell debris was pelleted by centrifugation (40,900 \times g for 30 min), the clarified cell lysate was subjected to a 40% ammonium sulfate fractionation. The suspension was centrifuged (40,900 \times g for 30 min), and the resulting pellet was resuspended in 1 M ammonium sulfate, 20 mM Tris, pH 7.5, 10 mM BME. The dissolved pellet was loaded onto a 50-ml phenyl-Sepharose 6 Fast-Flow HS column (Amersham BioSciences, Piscataway, NJ) equilibrated with buffer C (1.5 M ammonium sulfate, 20 mM Tris, pH 7.5, and 10 mM BME). Protein was eluted with a 10-column-volume gradient to 100% buffer A. Fractions containing SARS-CoV PLpro were pooled and diluted fivefold with buffer A and loaded onto a 50-ml Q-Sepharose Fast-Flow column (Amersham BioSciences, Piscataway, NJ) equilibrated with the same buffer. A 10-column-volume gradient to 100% buffer B (0.5 M NaCl, 20 mM Tris, pH 7.5, 10 mM BME) was used to elute the protein. SARS-CoV PLpro fractions were pooled, diluted fivefold with buffer A, and loaded onto a Mono Q 10/10 column (Amersham BioSciences, Piscataway, NJ). PLpro eluted under the same conditions as the Q-Sepharose column. Pure SARS-CoV PLpro fractions were exchanged into buffer A containing 20% glycerol, concentrated to approximately 20 mg/ml, flash-frozen in dry ice-ethanol, and stored at -80°C. Site-directed mutants of SARS-CoV PLpro enzymes were expressed, purified, and stored in the same manner.

Transfection and immunoprecipitation of SARS-CoV PLpro constructs. Expression of SARS-CoV PLpro constructs was performed as previously described (17). Briefly, HeLa-MHVR cells were infected with recombinant vaccinia vTF73 expressing T7 polymerase and transfected with plasmid DNAs pSARS-CoV PLpro and/or pNSP1-3* substrate using Lipofectamine (Invitrogen). Proteins were metabolically labeled using 100 μ Ci/ml Trans-³⁵S label for 4 h at 37°C. Cells were harvested by scraping into 0.3 ml of lysis buffer A (4% sodium dodecyl sulfate [SDS], 3% dithiothreitol, 40% glycerol, 0.065 M Tris, pH 6.8). Cell lysates were diluted in 1 ml of radioimmunoprecipitation assay buffer and immunoprecipitated with specific antibodies and protein A-Sepharose beads (Amersham Bioscience, Piscataway, N.J.). The following antibodies were used: rabbit polyclonal antibody anti-R1 to detect SARS-CoV nsp1 and anti-R3 to detect SARS-CoV nsp3, including SARS-CoV PLpro (17). Mouse monoclonal anti-V5 (Invitrogen) was used to detect epitope-tagged constructs as indicated. Immunoprecipitates were resolved by SDS-polyacrylamide gel electrophoresis (SDS-PAGE).

Fluorescence and FRET assays for enzyme kinetics. All assays were performed in 50 mM HEPES, pH 7.5, in a 500- μ l cuvette maintained at 25°C via a Peltier sample holder. The rates of the reaction were monitored using a Cary Eclipse Fluorescence Spectrophotometer (Varian, Palo Alto, CA). The fluorescence extinction coefficients of both fluorescent substrates were determined using the endpoint method as follows: an excess of SARS-CoV PLpro enzyme was added to various concentrations of substrate, and reactions were allowed to go to

completion. The final fluorescence values after blank subtraction were plotted against substrate concentration. The slope of the resulting line yielded a fluorescence extinction coefficient of each substrate under the conditions of the assay. Assays to determine peptide cleavage velocities were fixed-time-point assays, using various concentrations of the fluorescent resonance energy transfer (FRET) peptide substrate (E-EDANS)RELNGGAPI(K-DABCYL)S [EDANS, 5-((2-aminoethyl) amino) naphthalene-1-sulfonic acid; DABCYL, 4-((4-dimethylamino) phenyl) azo benzoic acid] (Sigma-Genosys, The Woodlands, TX) and 1 μ M purified SARS-CoV PLpro. The reactions were diluted to a 2 μ M final peptide concentration after initiation but immediately prior to acquiring fluorescence measurements (excitation λ , 340 nm; emission λ , 510 nm) to avoid inner-filter effect contributions. Several time points were taken for each peptide concentration to ensure that data points were representative of initial velocity measurements. Readings were corrected for dilution and plotted against peptide concentration. Since all peptide concentrations tested were well below the K_m value, as demonstrated by the linearity of the velocity versus peptide concentration relationship, data points were fit to the following equation: $v/[E]_{\text{Total}} = k_{\text{app}}[S]$ to determine the pseudo first-order rate constant k_{app} assuming that $[S] \ll K_m$. $[E]$ and $[S]$ are the concentrations of enzyme and peptide substrate, and v is the initial rate of the reaction. The same measurements were repeated for purified PLpro mutants. Kinetic assays to determine deubiquitination rates contained varying or fixed concentrations of the fluorogenic substrate ubiquitin-7-amino-4-methylcoumarin (AMC; BostonBiochem, Cambridge, MA) and 60 nM wild-type or mutant PLpro. Fluorescence was monitored continuously (excitation λ , 380 nm; emission λ , 460 nm). The initial velocity measurements were plotted against the ubiquitin-AMC concentration and fit to the equation above to determine the pseudo first-order rate constant.

In vitro assay for deubiquitination. A previously described procedure (21) was modified and used to examine whether the SARS-CoV PLpro has deubiquitination activity. Briefly, an equal amount (2.0 μ g) of purified SARS-CoV PLpro wild-type protein or mutant (D1826A and C1651A) protein was incubated with 4.0 μ g of the diubiquitin substrate (diubiquitin WT Chains, K48-linked; Boston Biochem) at 37°C for 5 to 60 min in 20 μ l of reaction buffer containing 25 mM Tris, pH 8.0, 100 mM NaCl, 100 μ g/ml bovine serum albumin, and 2 mM dithiothreitol. The reaction was stopped by the addition of 20 μ l of 2 \times SDS sample buffer, analyzed by electrophoresis on a 10 to 20% polyacrylamide gel (Criterion, Bio-Rad), and visualized by Coomassie blue staining.

RESULTS

Identifying a catalytic core domain of SARS-CoV PLpro. To identify a catalytic core domain of SARS-CoV PLpro, we performed sequential deletion analysis on pPLpro1541-2204, which we had previously shown to express an active protease in *trans*-cleavage assays (17). Initially, we deleted 280 amino acids from the C-terminal end of the construct to generate pPLpro1541-1924 (Fig. 1A). This construct was used as the parental construct for subsequent deletions of 20 to 30 amino acids from either the N- or C-terminal end of the PLpro domain. We tested each construct for expression of PLpro (Fig. 1B) and for protease activity in the *trans*-cleavage assay (Fig. 1C). We found that each construct expressed a PLpro domain of the expected size, and similar amounts of the PLpro product were immunoprecipitated by polyclonal antiserum that recognizes the SARS-CoV PLpro domain (Fig. 1B, lanes 1 to 10). When these constructs were cotransfected with plasmid DNA expressing the substrate NSP1-3*, we found that only 5 of the 10 expressed PLpro proteins were enzymatically active and able to cleave the substrate to produce the nsp1 product (Fig. 1C, lanes 1 to 3 and 6 to 7). Of these five functional PLpro domains, we found that the three C-terminal deletion constructs displayed more robust protease activity compared to the two N-terminal deletion products, as determined by monitoring the reduction of the NSP1-3* substrate. To determine if both C- and N-terminal regions could be truncated, we generated the double-deletion construct pPLpro1602-1855. However, this PLpro domain was no longer active in the *trans*-cleavage assay

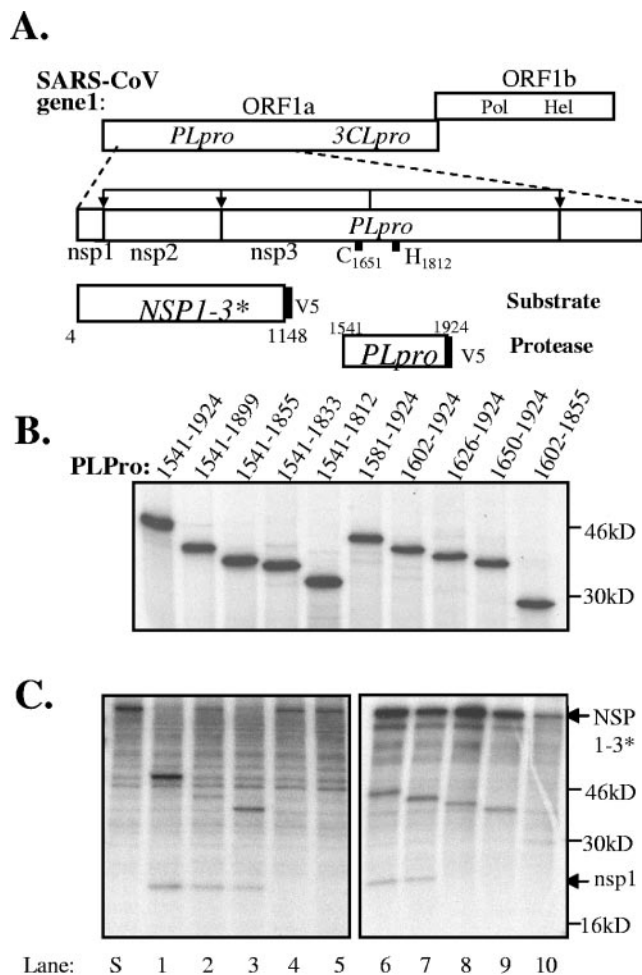


FIG. 1. Defining a core SARS-CoV PLpro domain using a *trans*-cleavage assay. (A) Schematic diagram of constructs generated to identify an active core domain of SARS-CoV PLpro. Starting with the fragment from residues 1541 to 1924, successive deletions of 20 amino acids were made from the C-terminal and N-terminal ends. The catalytic cysteine (C1651) and histidine (H1812) residues are indicated (17, 54). The constructs are designated by the residues at which they begin and end. (B) Expression of SARS-CoV PLpro deletion constructs. SARS-CoV PLpro deletion constructs were expressed via vaccinia-mediated T7 expression in HeLa cells. The proteins were radiolabeled with Trans-³⁵S, immunoprecipitated with antibody anti-R3, and resolved by SDS-PAGE. (C) *trans*-cleavage assay to assess PLpro activity. SARS-CoV PLpro deletion mutants were coexpressed with substrate NSP1-3* as shown, via vaccinia-mediated T7 expression in HeLa cells. The proteins were radiolabeled with Trans-³⁵S, immunoprecipitated with antibody anti-R1, which precipitates the uncleaved precursor NSP1-3* and cleavage product nsp1. Products were analyzed by electrophoresis on SDS-10% polyacrylamide gels and visualized by autoradiography. ORF, open reading frame.

(Fig. 1B, lane 10). Overall, we identified PLpro1541-1855 as a core catalytic domain of PLpro that retains robust protease activity in the *trans*-cleavage assay.

Comparison of coronavirus papain-like protease domains. To identify critical amino acid residues within the PLpro core domain, we compared the SARS-CoV PLpro1541-1855 amino acid sequence with the core papain-like protease domains of eight other coronaviruses (Fig. 2). Seven of these coronaviruses (MHV strain JHM, bovine CoV [BCoV], HCoV-HKU1,

SCoV PLp1541 -----EVKTIKVF---TTVDN--T--N---LHTQLVDMDSM<2>---GQQF-G<28>DITLRSE--A--FE---YYH
MHVJ P2 1606 -----LANKVDVL---CTVDG--V--N---FRSCCVAEGE<2>---GKTL-G<32>DLVAVKD--A--FG---F--
BCoV P2 1562 -----LDKVDIL---LTVDG--V--N---FTNR.FVPVGE<2>---GKSL-G<26>--DNLSSDLDKA--VR---SSF
OC43 P2 1562 -----LDKVDIL---LTVDG--V--N---FTNR.FVPVGE<2>---GKSL-G<26>--DNLSSDLDKA--VR---SSF
HKU P2 1647 L-----LAKKIDVL---LTVDG--V--N---FKSISLTVGE<2>---GKIL-G<29>LSLADIS--A--VQ---SSF
229E P2 1592 VGEKAA--EAKVITIK---VTEGD--V--N---VHDVTVTDDK<2>---EQQV-G<28>VDWVEFY--G--FKDAVTF
TGEV P2 1479 -----QTIENF<8>VTEDN--V--N---HERVSVSFDK<2>---GEQLKG<26>IDI---D--W--QA---HYG
IBV PLp1165 QEHDYFDVTCQKQTIY---LTEDG--V--K---YRSIVLKPGE<2>---G-QF-G<25>TDI---KS--I--LE---YYG
NL63 P2 1569 NVMDVNDCFKNDNVVLK---ITEGD--I--N---VKDVVVESSK<2>---GKQL-G<16>TDTVLSV--A--PE---VDW
TGEV P1 983 INITADEKSEVSASSE--EEVES--VEED--PENEIVEASEG<5>---SQEE-V<23>DD-----P---WAA
229E P1 944 GDWDS--FCKTIQSA--LSVSVSCYV--N--LPTYI--<1>---DEE-G<28>---IEAD--V--VD---QVE
NL63 P1 952 -----TSAMN--VI-G---QHILQPFYI<1>---DEEG-GY<35>DDBVREE--V--DI---IEQ
HKU P1 951 -----VTGDN--D--DEDVVTGDNDDDEDV<2>---GDND-D-<-->DDVDDIE--SIYDFD--TYK
MHVJ P1 1010 SQT-----PIASAE--TEVGE--A-C--DREGIAEVKA<2>CADALDA-C<28>DKTYE-D--V--LA--FDA
OC43 P1 964 ---P-----EDDDFLEE---SDVEE--D-C--VEGETDLTV<2>---AGQ-----<23>VETSDSQ--V--EE---DVE
BCoV P1 964 ---P-----EDDDFLEE---SGVEE--D-D--VEGETDLTV<2>---AGE-----<23>VETSDSQ--V--EE---DVE

ScOv PLp1614 TL--D--ESFLGRYMSALN--HTKWKWFP--Q--VGGLTIS--KWADNN--CYLSSVLLALQOLEVKNAPALQEAAYRARAG
MHVJ P2 1682 ---D--EPQLLKYYSMLG--MC-KWQVV--V--CGNYFAF--KQSNNN--CYINVACLMLQHLKLPKQWRRPGNEFRSG
BCoV P2 1634 NF--D--QKELLAYNMLV--NC SKWQVV--F--NGKYFTF--KQANNNC--FVNVSC LMLOSLNLKFKI VQWQEAWLEFRSG
OC43 P2 1634 NF--D--QKELLAYNMLV--NC SKWQVV--V--NGKYFTF--KQANNNC--FVNVSC LMLOSLHLTKFKI VQWQEAWLEFRSG
HKU P2 1721 GF--D--QQOLLAYNFLT---VCKWSVV--V--NGPFFSF--EQSHNN--CYNVAC LMLOHINLKNKQWQEAWYFRAG
229E P2 1675 TV--D--HSAFAYESAV-----VNGIRVL--KTSDDNC--WVNAVCTAL OYSKPHFISQGLDAAWNKFKVLG
TGEV P2 1554 FR--D--AA--AFSASS--HD--AYKFE--V--VTHSNFIVHKQTDNNC--WINAICLALORLQKWFPGVRGLWNEFLER
IBV PLp1240 -L--D--AQKYVIYLTQL--AQKWNVQ--Y--RDNFLIL--EWRDGN--CWISSAIVLLQAKIRFKG-FLTEAWAKLLGG
NL63 P2 1639 VA--F--YGEKAALFASL--DVKPYGYP--NDFVGGFRVL--GTTDNN--WVNVATCIILOYLKPTFKSKGLNVLNKFVTG
TGEV P1 1059 AV--D--VQEAQFNPSL---PPFKTT--N--LNGKIIL--KQGDNN--WINACCYQLOAFDF-FN---NEAWEKFKKG
229E P1 1015 EV--N--SFDIETVDVKH--DVSFFEMFEE--LNGKLIL--KQLDNN--WVNSVMIQIOLTKGLLDGDYAO---FF--KMG
NL63 P1 1028 PF--E--EV--EHLVSIK--QPFSSFR--D--ELGVRVL--DQSDNN--WISTTLVQLOLTKGLLDSIEMQ---LKFVG
HKU P1 1120 AL<7>N--DALFVSYGSSVE--TETTYFK-----VNGWSP--TITHTNC--WLRSVLLVMOKLFFKFDLAIENMWSLYKVG
MHVJ P1 1087 IY--S--ETLSAFYAVPSD--ETHE-----K--VCGFYSP--AIERTNC--WLRSTLVMSOPLFKDLSMOKLWLSYKAG
OC43 P1 1031 MS--D--DFVDLSVIQDYENVCFEYFYTEPEFV--K--VLGLYVP--KATRNN--WLRSVLAVMOKLPCQFKDKNLDLWVLYKQQ
BCoV P1 1031 MS--D--DFADLSVIQDYENVCFEYFYTEPEFV--K--VLDLYVP--KATRNN--WLRSVLAVMOKLPCQFKDKNLDLWVLYKQQ

zinc-binding cys * *
SCoV PLp1683 DAANFCALILAY--SNKTV--GELGDVRETMTHLLOHANLESAKRVLN--V-V--KHG--SOK-TTTLTGVEA--VMYMGTLSDYDNL
MHVJ P2 1748 KPLRFVSLVLAK--GSFKF--NEPSDSTDFIRVFLREADLSGATCDLE--F-I--OK--SVK-QEQRKGVDA--VMHFGTLDKSGL
BCoV P2 1703 RPAREVSLVLAK--GGFKF--GDPADSRDFLRVVSQVLDLTAICDFE--I-A--CK--SVK-QEQRKGVDA--VMHFGTLDKSGL
OC43 P2 1703 RPAREVSLVLAK--GGFKF--GDPADSRDFLRVVSQVLDLTAICDFE--I-A--CK--SVK-QEQRKGVDA--VMHFGTLDKSGL
HKU P2 1789 RHRLVALVLAK--GHFKF--DEPSDATDFIRVFLKQADLSGAICEL--L-I--C--DG--SJK-QESRVGVDA--VMHFGTLDKSGL
229E P2 1733 DVEIFVAFVYV--ARLMK--GDKGDAEDTITKLSKLANEAQVLEH--Y-SS--VE--D--AKFKMSVASINS-AIVCASVTRDGL
TGEV P2 1620 KTOGFVHMLYHI--SGVKK--GEPGDA-E LMLHKLGDMLDNDCEIIVTHTT-A--D--R--AK--F--VE---KFVG PVVAAPL
IBV PLp1305 DPTDFVAVCYAS--CTAKV--GDFSDANWLLANLAEHFDADYTNAFLLKRV-S--C--N--G--IK--SYELRGLA--CQPPVRAATNLLHF
NL63 P2 1710 DVGPFVFSFIYFI--TMSK--GQKGADEEALSSEYLSISDITVLEQ--YST--D--I--C--K--T--SVVVEKAS-AIVCASV---L
TGEV P1 1120 DVMDFVNLCAAA--TTLAR--GHSGDAEYLLLEMLN--DYSTAKIVLA--A-K--C--G--SEK-EIVL---ER-AVFKLTPLESF
229E P1 1082 RVAKMIERCYTA--EQCIR--GAMGDVGLCMYRLK--DLHTGFMVMD--Y-K--C--T--SG--RLEESG--A-VLFC-TPTKCAF
NL63 P1 1087 KVDSIVQKCYEL--SHLIS--GSLGDSGKLLSELLEK--YTCSITFE--M-S--O--D--G--SK--FDDQVG---CLFWIMPYTKL
HKU P1 1193 YNQSFDYDLT--IPKAI VLPQGGFVADFAYWFLNQFDINA--YAN--W-C--CL--K--G--F--SFDLNGLDA-LFFYGD--I
MHVJ P1 1152 YDQCFVDFKLVKS--APKSIILPQGGYVADFAYWFLNQ--S--SFKVHAN--W-R--CL--K--G--L--K--LQGLDA-VFFYGDV----
OC43 P1 1106 YSOLFVDTLVNKPANIVL--PQGGYVADFAYWFLTLCDWQC--VAY--W-K--CL--K--G--DL--ALKKGLDA-MFFYGDV----
BCoV P1 1106 YSOLFVDTLVNKPANIVV--PQGGYVADFAYWFLTLCDWQC--VAY--W-K--CL--K--G--DL--ALKKGLDA-MFFYGDV----

zinc-binding cys * *
SARS PLp1757 -KT-GVSIHVM--GRDAT-----QYLQV--QESS--EV--MMS--A---P--PAEYKLOQ--GTFLCANE
MHVJ P2 1821 -VK-GYNIACIT--GDKLV-----HCTQ--FNVP--FL--ICS--N---T--PEGKLPD--DV--VAANI
BCoV P2 1776 -EI-GYTVDCSP--GKKLI-----HCVR--FDVP--FL--ICS--N---T--PASVKLPK--GVG--SANI
OC43 P2 1776 -EI-GYTVDCSP--GKKLI-----HCVR--FDVP--FL--ICS--N---T--PASVKLPK--GVG--SANI
HKU P2 1862 -FN-GYKIGCNAGR--I--VHCTK--LNVP--FL--ICS--N---T--PLSKDLPD--DV--VAANM
229E P2 1808 -QV-GY--CVH--GIKYY-----SRVRS--VRGR--AI--IVS--VEQLEP--CAQSRLLS--GVAYTA
TGEV P2 1778 -AIHGTDDETCVH--GVSVN-----VKVTQ--IKGT--VA--ITSLIG--P--I--IGE VLEA--TGICY--
IBV PLp1381 -KT-QYSNCPTE--GANNT-----DEVIE--ASLP--YL--LLF--A---TDGPATVDCDEDAVGTVV---
NL63 P2 1777 -KD-GCDVGFDP--HRHKL-----RSRVK--FVNG--RV--VIT--N---V--GEPIISQP--SKLLNGIA
TGEV P1 1188 -NY-GVGDGDMQ--VNTCR-----FLSVE--GSGV--FVHDILS--K--Q--T--PEAMFVV--KPMHA-V
229E P1 1150 -PY-GTLLNCNA--PRMCT-----IRQLQ--GTII--FV--QOK--P---E--PVNPFVSV--KVPVCSSI
NL63 P1 1157 FQK-GEC--CLP--HKMQT-----YKLVV--MKG--GV--FVQ--D---PA--PIDIDAFP--VKPICSSV
HKU P1 1260 -----VSHVCKC--GHNMT-----LIAAD--LPCTLHFS--LFD--D---N--FCAFC--KIFIAACA
MHVJ P1 1219 -----VSHMCKC--GNSMTLLSADIPYTFDFVGRDDK--FC--AFY--T---P--R--KVFRA---ACAVD
OC43 P1 1172 -----VSHVCKC--GE--S-----MVLID--VDVP--FT-----AHFALKD--KLFCAFIT
BCoV P1 1172 -----VSHVCKC--GE--S-----MVLID--VDVP--FT-----AHFALKD--KLFCAFIT

DUB signature seq * catalytic his * catalytic asp
SCoV PLp1804 YIT--GNYQCGH--Y--T--HITAKETLYR---IDGAHLT--KMSEYK<16>IKP-----%ID
MHVJ P2 1867 FT--GG-SVGH--Y--T--HVKCKPKYQL---YDACNVS--KVSEAK<22>YY-----32
BCoV P2 1822 EK--GD-KVGH--Y--V--HVKCEQSYQL---YDASNVK--KVTDVT<22>YY-----31
OC43 P2 1822 EI--GD-KVGH--Y--V--HVKCEQSYQL---YDASNVK--KVTDVT<22>YY-----30
HKU P2 1907 FM--G-VGVGH--Y--T--HLKCGSPYQH---YDACSVK--KYTGVS<19>LTNY-----28
229E P2 1857 FS--GPVDKGH--Y--TVYDTAKKSMY---DGRFV--KHDLSL<18>VK-----22
TGEV P2 1736 YS--G--NRNGH--Y--T--YYDNRNGLV---VDA--E--KAYHEN<16>KKPQAEERPKNCAFNK--22
IBV PLp1490 EV--GSTNSGCH--Y--T--QAAGQ---A---FDNLAKD--RKFGK<17>SLPV-----22
NL63 P2 1825 YITFS--GSDFNH--Y--VVYDAANNNAVY---DGARLF--SSDLSL<16>VPTIVSEK-----21
TGEV P1 1237 YIT--GTTQNGH--Y--M--VDDIEHGYC---VDGMGIK--PLKK-R<16>EKPKQEFKVEKVEQQ--21
229E P1 1197 FR--GAVSCGH--Y--QT--NIYSQNLK---VDGFGVN--KIQPWT<24>IKNTVD-----20
NL63 P1 1204 YL--GVKGSGH--Y--T--QTNLYSFNKALDGFVGF--DIK--N<22>VKPFVAVYKNNK-----19
HKU P1 1306 VD--NVNC--H--S--V--AVIGDE---Q---IDGKFVT--KFSGDK<23>ITPNVCF-----20
MHVJ P1 1267 VN-----DCHS--M--A--VVDGKQ---IDGKVVT--KENGDK<25>ITPNVCF-----18
OC43 P1 1199 KR--IVYKAAC--V--V--DVNDSHSMAV---VDGKQIDDRITSTIT<28>ITPNVCF-----18
BCoV P1 1199 KR--SVYKAAC--V--V--DVNDSHSMAV---VDGKQIDDRITSTIT<28>ITPNVCF-----18

Downloaded from http://jvi.asm.org/ on March 29, 2015 by guest

TGEV, HCoV-NL63, HCoV-229E, and HCoV-OC43) encode two papain-like protease domains, termed either PLP1 and PLP2, or PL1pro and PL2pro. Two coronaviruses, SARS-CoV and aIBV, encode only one papain-like protease domain, which we term PLpro. For our analysis, we selected the amino acid sequences of each virus that would be analogous to the SARS-CoV PLpro minimal domain (a 316-amino-acid region, with 110 amino acids upstream of the putative catalytic cysteine residue and 206 amino acids downstream). The multiple sequence alignment revealed that although the overall identity of amino acids in the coronavirus papain-like protease domain is low (18 to 32%), the amino acids likely to participate in the catalytic core are highly conserved (Fig. 2, boxed sequences). Previous experimental evidence and computer modeling suggested that coronavirus papain-like proteases possess a Zn²⁺ binding domain that connects the left- and right-hand domains of a papain-like fold and that protease activity is mediated by a Cys-His catalytic dyad (19, 26, 63). Interestingly, both our analysis and the recent modeling of Sulea and coworkers (53) identify an additional and conserved residue, D1826, which may also be important for PLpro activity (Fig. 2, boxed in red). We hypothesize that coronavirus papain-like proteases, like cellular papain-like proteinases, may employ a Cys-His-Asp catalytic triad that is assisted by a conserved residue (usually Q/N) occupying the oxyanion hole (6, 23, 37, 51). To determine if D1826 and the putative zinc-binding residues are important for protease activity, we performed site-directed mutagenesis and changed the nucleotide sequence to code for alanine at the selected sites. The resulting PLpro proteins were tested for activity in the *trans*-cleavage assay (Fig. 3). As predicted, we found that alanine substitution of the conserved residues (C1651, D1826, and putative zinc-binding residues C1729, C1732, C1764, and C1766) resulted in the complete loss of PLpro activity as observed via *trans*-cleavage assays. In contrast, alanine substitution of a nonconserved cysteine (C1688) residue did not affect protease activity. Overall, these results support the hypothesis that the zinc-binding domain is important for the maintenance of the active site and that coronavirus papain-like proteases may exploit a Cys-His-Asp catalytic triad similar to cellular papain-like proteases.

Sulea and coworkers also predicted that a tryptophan residue in position 1646 may serve as a putative oxyanion-hole residue for SARS-CoV PLpro. The oxyanion-hole is usually filled by a glutamine or asparagine residue, and we hypothesize that the highly conserved glutamine residue downstream from the catalytic cysteine (residue 1661 in SARS-CoV PLpro) may function as an oxyanion-hole residue (Fig. 2, boxed in red). However, we found that alanine substitution of Q1661 did not

abolish SARS-CoV PLpro activity in the *trans*-cleavage assay, suggesting that this residue does not play a critical role in processing (data not shown). Ultimately, structural data will be essential for defining the SARS-CoV PLpro active site.

Our bioinformatics analysis was also consistent with the prediction of Sulea et al. (53) that suggested that coronavirus PLpro domains have a signature, substrate-binding site that may support deubiquitinating activity. By mining the current Protein Data Bank, Sulea and coworkers predicted that the SARS-CoV PLpro sequence from K1632 to E1847 may have a structure similar to the catalytic core domain of the cellular protein USP7, which is also known as HAUSP. This cysteine protease has been shown to have deubiquitinating activity (21). Molecular modeling of SARS-CoV PLpro suggests that this protease, like HAUSP and other deubiquitinating enzymes (DUBs), may recognize substrates with the sequence LXGG. Sulea and coworkers noted that the model predicts that significant occlusions of the S₁ and S₂ subsites account for the strict specificity for the predicted diglycine substrate. Furthermore, they noted that these “structural signatures for strict specificity,” which we term the “DUB signature sequences,” were present in HCoV-229E PL1pro and PL2pro and MHV PLP2, but not MHV PLP1. Our analysis extends these observations, and we noted that 12 of the 16 coronavirus papain-like protease domains retain the conserved signature sequence (Fig. 2, boxed in blue). Only four PL1pro domains (HCoV-HKU1 PLP1, MHV PLP1, HCoV-OC43 PLP1, and BCoV PLP1) do not retain the signature sequence and therefore would not be predicted to exhibit deubiquitinating activity. To determine if the putative “DUB signature residues” are essential for SARS-CoV PLpro activity, we generated alanine substitution mutants and tested them for activity in the *trans*-cleavage assay (Fig. 3, lanes 10 and 11). As predicted, replacement of the Y1804 or Y1813 resulted in a loss of protease activity. These results provide the first experimental evidence that two of the residues in the DUB signature sequences are important for maintaining the active site.

Purification of SARS-CoV PLpro. Ultimately, our goal is to purify an active form of SARS-CoV PLpro for use in a high-throughput assay to screen for inhibitors that block protease activity, as well as for crystallization and X-ray structure determination. As a first step toward these goals, we expressed SARS-CoV PLpro1541-1855 in *E. coli* BL21(DE3) cells, purified the protein to homogeneity, and developed a FRET-based peptide cleavage assay to measure the kinetics of SARS-CoV PLpro activity. The purification consisted of a combination of hydrophobic interaction and anion exchange chromatography and resulted in the purification of a protein that resolved as a

FIG. 2. Multiple sequence alignment of coronavirus papain-like protease domains. The papain-like protease domain amino acid sequences (either one domain termed PLpro or two domains termed P1 and P2) of nine different coronaviruses (SARS CoV, MHV-JHM, BCoV, HCoV-OC43, HCoV-229E, HCoV-NL63, TGEV, HCoV-HKU1, and aIBV) were aligned using the ALIGN program (SciEd). The amino acids from 1541 to 1855 of SARS-CoV PLpro, experimentally determined as the core domain, were used as a reference sequence. Amino acid numbers are indicated on the left. The regions of identity are highlighted in yellow. Predicted or experimentally determined catalytic cysteine residues, catalytic histidine residues, and cysteine or histidine residues essential for binding zinc are indicated by black boxes. The predicted catalytic aspartic acid residue and putative oxyanion glutamine residue are boxed in red. Residues proposed to be part of the substrate binding site for deubiquitination are boxed in blue. Accession numbers are as follows: SARS-CoV Urbani strain, AY278741; MHVJ (for MHV-JHM), NC_001846; BCoV, NC_003045; HCoV-OC43, AY585228; HCoV-229E, X69721; HCoV-NL63, NC_005831; TGEV, Z34093; aIBV, NC_001451; HCoV-HKU1, NC_006577.

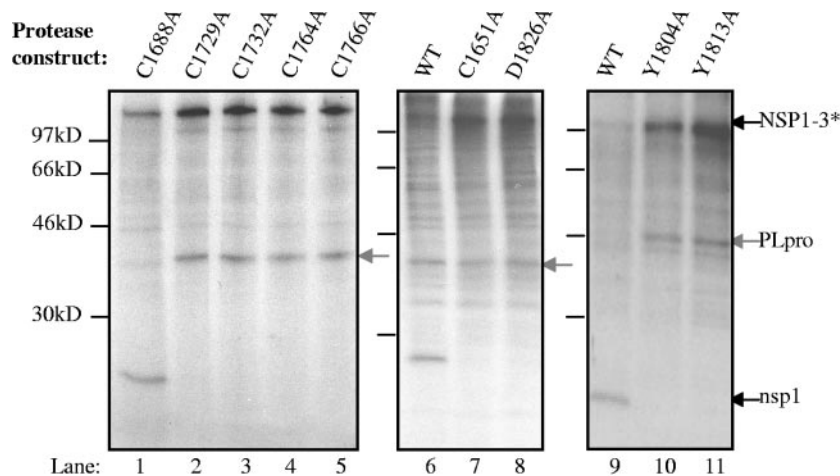


FIG. 3. Identifying residues essential for proteolytic activity of SARS-CoV PLpro. SARS-CoV PLpro constructs encoding the wild-type sequence or specific alanine substitutions were coexpressed with substrate NSP1-3* as described in the legend of Fig. 1C to identify residues essential for SARS-CoV PLpro activity. The site of the alanine substitution is indicated above each lane. WT, wild type.

single protein of approximately 35 kDa (Fig. 4A). A typical purification of SARS-CoV PLpro from 3 liters of bacteria cell culture yields roughly 90 mg of wild-type SARS-CoV PLpro protein. We also expressed and purified SARS-CoV PLpro proteins containing an alanine substitution at putative catalytic residues, SARS-CoV PLproC1651A and SARS-CoV PLpro D1826A. However, both PLpro mutants produced significantly lower yields due to reduced levels of expression in the soluble fraction. Approximately 10 mg of pure protein was obtained for each mutant. Interestingly, a third mutant, SARS-CoV PLproC1732A, which encodes a substitution of a cysteine residue predicted to be critical for zinc binding, could only be expressed as insoluble inclusion bodies under several different expression conditions. As a result, the SARS-CoV PLpro C1732A mutant could not be purified using the established protocol. This may indicate that correct zinc binding is essential for proper folding and solubility of the SARS-CoV PLpro enzyme.

Kinetic analysis of SARS-CoV PLpro. Purified SARS-CoV PLpro wild-type and mutant proteins were used to determine the kinetic parameters of cleavage of two different substrates. The first substrate tested was a synthetic peptide derived from the nsp1/nsp2 and nsp2/nsp3 sequences that are preferred by PLpro1541-2204 (17). DABCYL and EDANS moieties on opposite ends of the 12-mer peptide, (E-EDANS)RELNGGAP I(K-DABCYL)S, allowed for easy detection of peptide hydrolysis in a FRET-based kinetic assay as described in Materials and Methods. The putative PLpro recognition site is underlined in the sequences. Proteolysis of the substrate results in fluorescence due to the release of the fluorophore from the proximity of the quencher. Wild-type SARS-CoV PLpro was highly active but could not be saturated with substrate even at the highest concentration of peptide tested, i.e., 400 μM (data not shown). Based on the observation that enzyme activity was linearly proportional to increasing concentration of the peptide substrate (Fig. 4B), the initial velocity measurements were plotted against substrate concentration to determine the pseudo first-order rate constant, k_{app} , for SARS-CoV PLpro activity (Fig. 4B) (k_{app} approximates k_{cat}/K_m for nonsaturable

enzymes). The pseudo first-order rate constant for wild-type SARS-CoV PLpro, calculated from rates obtained at different peptide concentrations was determined to be $(2.44 \pm 0.03) \times 10^{-2} \text{ min}^{-1} \mu\text{M}^{-1}$ (Table 1). The SARS-CoV PLpro active-site mutant, C1651A, was completely inactive with the peptide substrate. However, SARS CoV PLproD1826A, a putative catalytic triad mutant, was determined to be slightly active with approximately a 100-fold decrease in the k_{app} value, which is $(2.3 \pm 0.2) \times 10^{-4} \text{ min}^{-1} \mu\text{M}^{-1}$. These results are consistent with studies of other papain-like proteases and deubiquitinating enzymes, where it was shown that the cysteine residue plays an essential and critical role in the nucleophilic attack of the reaction and that the aspartic acid plays a significant, although not essential role, in orienting and/or stabilizing the substrate in the active site (23, 31).

Purified SARS-CoV PLpro was also tested for deubiquitinating activity in vitro using a commercially available fluorescent substrate, ubiquitin-AMC. As with the fluorescent peptide, saturation could not be achieved with the ubiquitin substrate at the concentrations assayed. Interestingly, SARS-CoV PLpro showed a strong preference for the ubiquitin substrate over the peptide substrate with a deubiquitinating activity that is 180-fold more efficient (k_{app} value of $4.48 \pm 0.11 \text{ min}^{-1} \mu\text{M}^{-1}$) than with the peptide substrate (Fig. 4B and Table 1). Indeed, SARS-CoV PLpro is considerably more active against the ubiquitin-AMC substrate than HAUSP ($k_{\text{cat}}/K_m = 13 \text{ min}^{-1} \text{ mM}^{-1}$ [21]). For both SARS-CoV PLpro and HAUSP enzymes, K_m values could not be determined, since saturation of the enzymes with peptide substrates could not be achieved (21). Therefore the k_{app} for SARS-CoV PLpro and the reported k_{cat}/K_m for HAUSP indicate that these enzymes have low affinities for the peptide substrates tested but substantial turnover rates. In contrast, the K_m values observed for several other ubiquitin C-terminal hydrolases family members are in the range of 1 to 3 μM , indicating that they have higher affinity for their substrates (10, 24, 30, 32). SARS-CoV PLproC1651A and PLproD1826A were also tested for deubiquitinating activity; PLproC1651A was again completely inactive, whereas PLproD1826A displayed only 1% the activity of

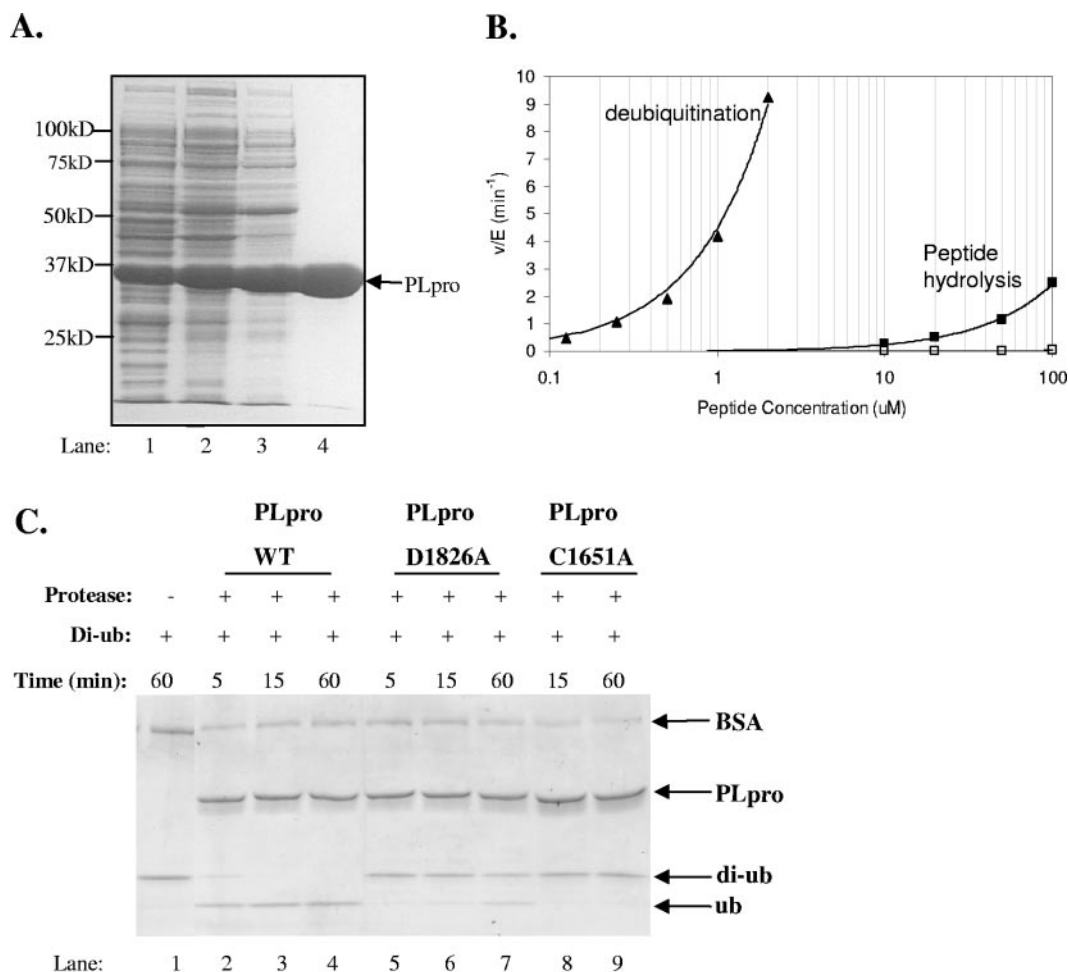


FIG. 4. Purification of SARS-CoV PLpro1541-1855 and in vitro assays for enzymatic activity. (A) Expression and purification of wild-type SARS-CoV PLpro. Samples (20 μg) from each stage of the purification were analyzed on an SDS-10% polyacrylamide gel and stained with Coomassie brilliant blue. Lane 1, soluble, crude cell lysate from *E. coli* BL21(DE3) cells expressing pET11a-SARS CoV-PLpro; lane 2, resuspended pellet of the 40% ammonium sulfate cut of the lysate; lane 3, pooled peak fractions from the phenyl-Sepharose column; lane 4, pooled peak fractions after elution from the Q Sepharose and Mono Q columns. (B) Kinetic assay of peptide hydrolysis and deubiquitination. The peptide hydrolysis (■) and deubiquitinating (▲) activity of wild-type SARS-CoV PLpro were tested at different concentrations of substrate in 50 mM HEPES, pH 7.5, at 25°C. Peptide hydrolysis reactions contained 1 μM enzyme, whereas deubiquitination assays contained 60 nM enzyme. PLproD1826A was also assayed for proteolytic activity against the fluorescent peptide substrate (□) under the same conditions listed for the wild-type enzyme. The data were fit to the equation $v/[E]_{\text{Total}} = k_{\text{app}} [S]$ by linear regression and then plotted as log [peptide] (peptide concentration) in order to see the differences in rates with the various substrates. (C) SARS-CoV PLpro cleavage of diubiquitin. Wild-type and alanine substitution mutants of SARS-CoV PLpro were tested for their ability to process diubiquitin in vitro. Purified proteins were incubated at 37°C with diubiquitin in a reaction buffer containing bovine serum albumin (BSA) for the times indicated. Cleavage products were analyzed by electrophoresis on a 10 to 20% gradient acrylamide gel and stained with Coomassie blue. The components in each reaction and the incubation time are indicated above each lane. ub, ubiquitin; di-ub, diubiquitin.

wild-type enzyme at the 0.5 μM concentration of ubiquitin-AMC substrate (data not shown).

To confirm these findings using an independent assay, we tested purified SARS-CoV PLpro wild-type and the C1651A and D1826A mutant enzymes for their ability to cleave a diubiquitin substrate (21). SARS-CoV PLpro enzymes were incubated with the diubiquitin substrate for 5, 15, and 60 min, and the products of the reaction were resolved by SDS-PAGE and visualized by staining with Coomassie blue (Fig. 4C). The diubiquitin substrate was efficiently cleaved by wild-type SARS-CoV PLpro, demonstrating its DUB activity. The catalytic cysteine mutant, PLproC1651A, was completely inactive in this assay, and PLproD1826A had a reduced but detectable

level of enzymatic activity. Thus, both fluorescence-based and protein-based assays provided experimental evidence for SARS-CoV PLpro DUB activity.

SARS-CoV PLpro recognizes and cleaves at the LXGG consensus cleavage site. Previous studies have predicted and provided some experimental evidence that SARS-CoV PLpro recognizes the consensus sequence LXGG at the three cleavage sites in the replicase polyprotein (16, 17, 54). Interestingly, this cleavage site is also the consensus cleavage site recognized by DUB enzymes such as HAUSP (21, 53). To determine if the predicted LXGG consensus site is indeed important for PLpro recognition and processing, we confirmed the location of each of the three cleavage sites and performed site-directed mu-

TABLE 1. Apparent k_{cat}/K_m (k_{app}) values for SARS-CoV PLpro wild type and mutants

SARS-CoV PLpro1541-1855 ^a	Deubiquitination k_{app} ($\text{min}^{-1}/\mu\text{M}^{-1}$) ^b	Peptide hydrolysis k_{app} ($\text{min}^{-1}/\mu\text{M}^{-1}$) ^c
WT	4.48 ± 0.11	$(2.44 \pm 0.03) \times 10^{-2}$
C1651A	No activity	No activity
D1826A	<1% activity of WT	$(2.3 \pm 0.2) \times 10^{-4}$

^a WT, wild type.

^b Substrate for deubiquitination: ubiquitin-AMC (cleavage site: LRGG-AMC). The PLpro recognition site is underlined, and the cleavage site is indicated by a -.

^c Substrate for peptide hydrolysis: (E-EDANS)RELNGG-API(K-DABCYL)S. See footnote b for explanation of underlining and -.

tagenesis to identify the critical determinants for PLpro recognition and processing. Cleavage sites were confirmed by subjecting the cleavage products generated in a *trans*-cleavage assay to Edman degradation to identify the amino-terminal residues (data not shown; methods as described in Kanjana-haluethai et al. [26]). As expected, the cleavage sites corresponded to the sites predicted for PLpro recognition and processing (54, 17) (Fig. 5). To identify the critical residues required for SARS-CoV PLpro recognition and processing, we performed alanine-scanning mutagenesis on the P6 to P2' at each cleavage site and used the *trans*-cleavage assay to monitor the effect of each substitution on PLpro processing. The products of each *trans*-cleavage assay were immunoprecipitated and resolved by SDS-PAGE as shown in Fig. 5. For each assay, the presence of the cleavage product indicates that the alanine substitution at that site had little or no effect on processing, whereas the absence of the cleavage product indicates that the alanine substitution resulted in a reduction in SARS-CoV PLpro recognition and processing. We found that for two of the cleavage sites, nsp1/nsp2 and nsp3/nsp4, alanine substitution of the leucine at P4 or glycine at P2 or P1 resulted in a marked reduction in protease recognition and processing. Thus, the consensus cleavage site LXGG is critical for SARS-CoV PLpro recognition and processing at these two sites. However, additional factors may also influence recognition and processing, as indicated by the SARS-CoV PLpro processing results at the nsp2/nsp 3 cleavage site. At this cleavage site, replacement of the leucine at P4 had little or no effect, and replacement of the glycines at P1 and P2 reduced, but did not abolish, processing. Interestingly, pulse-chase studies have shown that this site is also processed less efficiently in SARS-CoV-infected cells (17), which suggests that the NSP2-3 intermediate may play a role in viral replication. Thus, although the consensus LXGG sequence is important for SARS-CoV PLpro recognition and processing, additional factors may affect the efficiency of proteolytic processing at each cleavage site.

DISCUSSION

In this study, we show that SARS-CoV PLpro is a viral protease with DUB activity. We identified a core SARS-CoV PLpro domain of 316 amino acids that can process the amino-terminal portion of the SARS-CoV replicase polyprotein and can recognize and process ubiquitinated substrates. Using bioinformatic analysis, we identified conserved residues within this core and provided experimental evidence to support the hypothesis that SARS-CoV PLpro exploits a catalytic triad to

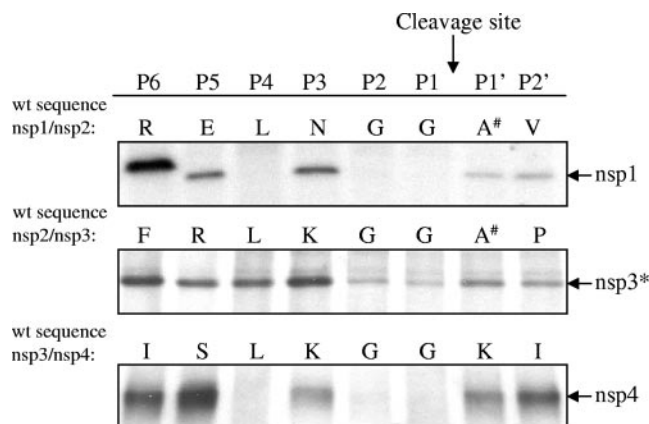


FIG. 5. SARS-CoV PLpro recognition and processing of LXGG consensus substrate cleavage sites. Alanine (or asparagine, indicated by #) substitutions were made at the P6 to P2' positions of the three SARS-CoV replicase polyprotein cleavage sites recognized by SARS-CoV PLpro: nsp1/nsp2, nsp2/nsp3 (in pNSP1-3* substrate) and nsp3/nsp4 (in pNSP*3-4 substrate [17]). The wild-type amino acid at each position is indicated above the gel. The substrate with the alanine substitution at each position was coexpressed with SARS-CoV PLpro1541-1855 in the *trans*-cleavage assay, and cleavage products were detected by immunoprecipitation. Products were analyzed by SDS-PAGE and autoradiography.

mediate proteolytic processing and DUB activity. Furthermore, SARS-CoV PLpro recognizes and cleaves substrates with the consensus sequence LXGG, which is also the consensus sequence processed by many cellular DUBs. These findings have important implications for the development of antiviral agents to PLpro and open new avenues of investigation concerning the role of a viral DUB activity in coronavirus replication and pathogenesis.

Current antiviral drug development is driven by two major approaches: high-throughput screening (HTS) of chemical compound libraries and rational drug design based on structural information. The identification of the core domain of PLpro and the development of *in vitro* assays for enzymatic activity described here will facilitate HTS for SARS-CoV PLpro inhibitors. The purified SARS-CoV PLpro core domain retained enzymatic activity *in vitro*, and kinetic studies indicated deubiquitinating activity was even more robust than hydrolysis of the 12-mer peptide substrate. It may be challenging to develop PLpro inhibitors that are specific for the viral protease, without blocking cellular DUBs. However, the structural differences in cellular DUBs suggest that these enzymes may be different enough to be selectively targeted. Further information from structural studies will be required to better understand and exploit any potential differences. We note that HTS using the other SARS-CoV protease, 3CLpro, has already led to the identification of many small-molecule inhibitors (7). In addition, HTS against SARS-CoV-infected cells has led to the identification of small molecules that target 3CLpro and block SARS CoV replication (59). The former approach could also be used to develop HTS assays for papain-like protease domains from other human coronaviruses such as the recently identified NL-63 (12, 55) and HKU-1 (58) and "common cold" coronaviruses OC43 and 229E (20). Finally,

the purification of PLpro is a critical first step toward obtaining structural information on this important therapeutic target.

This study also raises important questions concerning the role of a viral DUB activity in coronavirus replication and pathogenesis. Cellular DUBs are known to alter the fate of proteins targeted to specific pathways in the cell (1). Deubiquitination may change the fate of (i) ubiquitinated proteins bound for degradation in the proteasome (56), (ii) proteins modified by ubiquitin-like (UBL) modifications such as ISGylation (46), and (iii) proteins assembled in autophagosomes that are bound for degradation in lysosomes (48). Modulation of any of these pathways may have important implications on viral replication and pathogenesis. For example, HAUSP, the cellular DUB activated by herpesvirus infection, plays a dynamic role in the stabilization of p53. HAUSP can act directly to deubiquitinate p53, thereby stabilizing its tumor suppressor function (34). In addition, HAUSP acts on Mdm2, the ubiquitin ligase required to modify p53. In the absence of HAUSP, Mdm2 auto-ubiquitinates and is degraded, and p53 is stable in the cell (9, 33). This illustrates the dynamic effect that DUBs can have on protein stabilization. It is currently unclear if SARS-CoV PLpro specifically targets and stabilizes a cellular substrate. Further investigation is necessary to determine if specific substrates are recognized and stabilized by PLpro.

One interesting question is whether the SARS-CoV PLpro peptide hydrolysis and DUB activities can be separated. A better understanding of enzyme-substrate interactions is needed to identify distinct contact residues that may play a role in distinguishing one substrate from another.

Sulea et al. speculated that SARS PLpro DUB activity may function to inhibit innate immune responses such as conjugation with ISG15 (interferon [IFN]-sensitive gene 15), termed ISGylation (44, 53). ISG15, a ubiquitin-like protein, is induced in response to IFN- α/β . While the role of ISG15 is not entirely clear, it is conjugated to many targets, including JAK and STAT proteins, and this conjugation leads to suppression of cell proliferation (36). The adenovirus protease has been shown to have both deubiquitinating and "de-ISGylating" activity and recognizes the LXGG consensus site for removal of ISG15 (5). In addition, the influenza virus NS1 protein has been shown to inhibit the conjugation of ISG15, thereby counteracting this IFN-induced activity (62). Interestingly, recent studies indicate that SARS-CoV infection may escape IFN-mediated growth inhibition by blocking the activation of IFN regulatory factor 3 (49). The mechanisms and viral proteins required for this IFN-antagonistic effect are currently unclear. Experiments are currently under way to determine if ISG15 is activated and if levels of ISGylated proteins are altered in coronavirus-infected cells.

Another intriguing speculation is that SARS-CoV PLpro activity may be involved in subverting a normal cellular process known as autophagy to facilitate the assembly of DMVs, which are the site of coronavirus replication (14, 43). Autophagy is a cellular response to starvation conditions, whereby the cell recycles cytoplasmic components by enclosing them in double-membrane structures known as autophagosomes for delivery to lysosomes for degradation (48). At least 16 genes (termed Apg for autophagy-defective) and two UBL modification systems are required for autophagy in *Saccharomyces cerevisiae* (38, 39). In the first UBL system, Apg12 is activated by Apg7

and Apg10, which are E1-like and E2-like enzymes, respectively, of the ubiquitin system. Apg12 is then conjugated to Apg5, which is required for assembly of autophagosomes and viral DMVs (43). In the second UBL system, Apg8 is activated by E1-like and E2-like enzymes, Apg7 and Apg3, and is conjugated with phosphatidylethanolamine, making it a membrane-associated complex. Studies of both coronavirus and poliovirus replication complexes indicate that viral replicase proteins may assemble with intracellular membranes to form DMVs, which are the site of viral replication (13, 14, 40, 43, 45, 52). The mechanism for the assembly of the DMVs is not clear, but recent studies suggest that viral proteins may subvert the cellular autophagosomal machinery (22, 28, 43). For example, LC3, the mammalian homolog of yeast Atg8p, has been implicated in the assembly of viral DMVs since it colocalizes with coronavirus and poliovirus replication complexes (22, 43). We speculate that coronaviruses may exploit the cellular autophagy pathway for the assembly of the DMVs but then subvert the pathway by deubiquitination to prevent the maturation of the vesicles into degradative organelles. Experiments are currently in progress to test these hypotheses.

ACKNOWLEDGMENTS

We acknowledge the excellent technical assistance of Jonathan Moreira and Emily Richter.

This work was supported by Public Health Service research grant AI45798 (to S.C.B.) and P01 AI060915 (to S.C.B. and A.D.M.). N.B. was supported by Training Grant T32 AI007508.

REFERENCES

- Amerik, A. Y., and M. Hochstrasser. 2004. Mechanism and function of deubiquitinating enzymes. *Biochim. Biophys. Acta* **1695**:189–207.
- Bacha, U., J. Barrila, A. Velazquez-Campoy, S. A. Leavitt, and E. Freire. 2004. Identification of novel inhibitors of the SARS coronavirus main protease 3CLpro. *Biochemistry* **43**:4906–4912.
- Baker, S. C., C. K. Shieh, L. H. Soe, M. F. Chang, D. M. Vannier, and M. M. Lai. 1989. Identification of a domain required for autoproteolytic cleavage of murine coronavirus gene A polyprotein. *J. Virol.* **63**:3693–3699.
- Baker, S. C., K. Yokomori, S. Dong, R. Carlisle, A. E. Gorbalenya, E. V. Koonin, and M. M. Lai. 1993. Identification of the catalytic sites of a papain-like cysteine proteinase of murine coronavirus. *J. Virol.* **67**:6056–6063.
- Balakirev, M. Y., M. Jaquinod, A. L. Haas, and J. Chroboczek. 2002. Deubiquitinating function of adenovirus proteinase. *J. Virol.* **76**:6323–6331.
- Berti, P. J., and A. C. Storer. 1995. Alignment/phylogeny of the papain superfamily of cysteine proteases. *J. Mol. Biol.* **246**:273–283.
- Blanchard, J. E., N. H. Elowe, C. Huitema, P. D. Fortin, J. D. Cechetto, L. D. Eltis, and E. D. Brown. 2004. High-throughput screening identifies inhibitors of the SARS coronavirus main proteinase. *Chem. Biol.* **11**:1445–1453.
- Bonilla, P. J., S. A. Hughes, and S. R. Weiss. 1997. Characterization of a second cleavage site and demonstration of activity in *trans* by the papain-like proteinase of the murine coronavirus mouse hepatitis virus strain A59. *J. Virol.* **71**:900–909.
- Cummins, J. M., C. Rago, M. Kohli, K. W. Kinzler, C. Lengauer, and B. Vogelstein. 2004. Tumour suppression: disruption of HAUSP gene stabilizes p53. *Nature* **428**:486.
- Dang, L. C., F. D. Melandri, and R. L. Stein. 1998. Kinetic and mechanistic studies on the hydrolysis of ubiquitin C-terminal 7-amido-4-methylcoumarin by deubiquitinating enzymes. *Biochemistry* **37**:1868–1879.
- Donnelly, C. A., A. C. Ghani, G. M. Leung, A. J. Hedley, C. Fraser, S. Riley, L. J. Abu-Raddad, L.-M. Ho, T.-Q. Thach, P. Chau, K.-P. Chan, T.-H. Lam, L.-Y. Tse, T. Tsang, S.-H. Liu, J. H. B. Kong, E. M. C. Lau, N. M. Ferguson, and R. M. Anderson. 2003. Epidemiological determinants of spread of causal agent of severe acute respiratory syndrome in Hong Kong. *Lancet* **361**:1761–1766.
- Fouchier, R. A., N. G. Hartwig, T. M. Bestebroer, B. Niemeyer, J. C. de Jong, J. H. Simon, and A. D. Osterhaus. 2004. A previously undescribed coronavirus associated with respiratory disease in humans. *Proc. Natl. Acad. Sci. USA* **101**:6212–6216.
- Goldsmith, C. S., K. M. Tatti, T. G. Ksiazek, P. E. Rollin, J. A. Comer, W. W. Lee, P. A. Rota, B. Bankamp, W. J. Bellini, and S. R. Zaki. 2004. Ultrastructural characterization of SARS coronavirus. *Emerg. Infect. Dis.* **10**:320–326.
- Gosert, R., A. Kanjanahaluethai, D. Egger, K. Bienz, and S. C. Baker. 2002.

- RNA replication of mouse hepatitis virus takes place at double-membrane vesicles. *J. Virol.* **76**:3697–3708.
15. Guan, Y., B. J. Zheng, Y. Q. He, X. L. Liu, Z. X. Zhuang, C. L. Cheung, S. W. Luo, P. H. Li, L. J. Zhang, Y. J. Guan, K. M. Butt, K. L. Wong, K. W. Chan, W. Lim, K. F. Shortridge, K. Y. Yuen, J. S. Peiris, and L. L. Poon. 2003. Isolation and characterization of viruses related to the SARS coronavirus from animals in southern China. *Science* **302**:276–278.
 16. Han, Y. S., G. G. Chang, C. G. Joo, H. J. Lee, S. H. Yeh, J. T. Hsu, and X. Chen. 2005. Papain-like protease 2 (PLP2) from severe acute respiratory syndrome coronavirus (SARS-CoV): expression, purification, characterization, and inhibition. *Biochemistry* **44**:10349–10359.
 17. Harcourt, B. H., D. Jukneliene, A. Kanjanahaluethai, J. Bechill, K. M. Severson, C. M. Smith, P. A. Rota, and S. C. Baker. 2004. Identification of severe acute respiratory syndrome coronavirus replicase products and characterization of papain-like protease activity. *J. Virol.* **78**:13600–13612.
 18. Herold, J., A. E. Gorbalenya, V. Thiel, B. Schelle, and S. G. Siddell. 1998. Proteolytic processing at the amino terminus of human coronavirus 229E gene 1-encoded polyproteins: identification of a papain-like proteinase and its substrate. *J. Virol.* **72**:910–918.
 19. Herold, J., S. G. Siddell, and A. E. Gorbalenya. 1999. A human RNA viral cysteine proteinase that depends upon a unique Zn²⁺-binding finger connecting the two domains of a papain-like fold. *J. Biol. Chem.* **274**:14918–14925.
 20. Holmes, K. V. 2001. Coronaviruses, p. 1187–1203. *In* D. M. Knipe, P. M. Howley, D. E. Griffin, R. A. Lamb, M. A. Martin, B. Roizman, and S. E. Straus (ed.), *Fields virology*, 4th ed. Lippincott Williams & Wilkins, Philadelphia, Pa.
 21. Hu, M., P. Li, M. Li, W. Li, T. Yao, J. W. Wu, W. Gu, R. E. Cohen, and Y. Shi. 2002. Crystal structure of a UBP-family deubiquitinating enzyme in isolation and in complex with ubiquitin aldehyde. *Cell* **111**:1041–1054.
 22. Jackson, W. T., T. H. Giddings, Jr., M. P. Taylor, S. Mulinyawe, M. Rabinovitch, R. R. Kopito, and K. Kirkegaard. 2005. Subversion of cellular autophagosomal machinery by RNA viruses. *PLoS Biol.* **3**:0861–0871.
 23. Johnston, S. C., C. N. Larsen, W. J. Cook, K. D. Wilkinson, and C. P. Hill. 1997. Crystal structure of a deubiquitinating enzyme (human UCH-L3) at 1.8 Å resolution. *EMBO J.* **16**:3787–3796.
 24. Johnston, S. C., S. M. Riddle, R. E. Cohen, and C. P. Hill. 1999. Structural basis for the specificity of ubiquitin C-terminal hydrolases. *EMBO J.* **18**:3877–3887.
 25. Kanjanahaluethai, A., and S. C. Baker. 2000. Identification of mouse hepatitis virus papain-like proteinase 2 activity. *J. Virol.* **74**:7911–7921.
 26. Kanjanahaluethai, A., Jukneliene, D., and S. C. Baker. 2003. Identification of the murine coronavirus MP1 cleavage site recognized by papain-like proteinase 2. *J. Virol.* **77**:7376–7382.
 27. Kim, J. C., R. A. Spence, P. F. Currier, X. Lu, and M. R. Denison. 1995. Coronavirus protein processing and RNA synthesis is inhibited by the cysteine proteinase inhibitor E64d. *Virology* **208**:1–8.
 28. Kirkegaard, K., M. P. Taylor, and W. T. Jackson. 2004. Cellular autophagy: surrender, avoidance and subversion by microorganisms. *Nat. Rev. Microbiol.* **2**:301–314.
 29. Lai, M. M. C., and K. V. Holmes. 2001. Coronaviridae: the viruses and their replication, p. 1163–1185. *In* D. M. Knipe, P. M. Howley, D. E. Griffin, R. A. Lamb, M. A. Martin, B. Roizman, and S. E. Straus (ed.), *Fields virology*, 4th ed. Lippincott Williams & Wilkins, Philadelphia, Pa.
 30. Lam, Y. A., G. N. DeMartino, C. M. Pickart, and R. E. Cohen. 1997. Specificity of the ubiquitin isopeptidase in the PA700 regulatory complex of 26 S proteasomes. *J. Biol. Chem.* **272**:28438–28446.
 31. Larsen, C. N., B. A. Krantz, and K. D. Wilkinson. 1998. Substrate specificity of deubiquitinating enzymes: ubiquitin C-terminal hydrolases. *Biochemistry* **37**:3358–3368.
 32. Larsen, C. N., J. S. Price, and K. D. Wilkinson. 1996. Substrate binding and catalysis by ubiquitin C-terminal hydrolases: identification of two active site residues. *Biochemistry* **35**:6735–6744.
 33. Li, M., C. L. Brooks, N. Kon, and W. Gu. 2004. A dynamic role of HAUSP in the p53-Mdm2 pathway. *Mol. Cell* **13**:879–886.
 34. Li, M., D. Chen, A. Shiloh, J. Luo, A. Y. Nikolaev, J. Qin, and W. Gu. 2002. Deubiquitination of p53 by HAUSP is an important pathway for p53 stabilization. *Nature* **416**:648–653.
 35. Lim, K. P., L. F. Ng, and D. X. Liu. 2000. Identification of a novel cleavage activity of the first papain-like proteinase domain encoded by open reading frame 1a of the coronavirus avian infectious bronchitis virus and characterization of the cleavage products. *J. Virol.* **74**:1674–1685.
 36. Malakhov, M. P., O. A. Malakhova, K. I. Kim, K. J. Ritchie, and D. E. Zhang. 2002. UBP43 (USP18) specifically removes ISG15 from conjugated proteins. *J. Biol. Chem.* **277**:9976–9981.
 37. Menard, R., J. Carriere, P. Laflamme, C. Plouffe, H. E. Khouri, T. Vernet, D. C. Tessier, D. Y. Thomas, and A. C. Storer. 1991. Contribution of the glutamine 19 side chain to transition-state stabilization in the oxyanion hole of papain. *Biochemistry* **30**:8924–8928.
 38. Mizushima, N., T. Noda, T. Yoshimori, Y. Tanaka, T. Ishii, M. D. George, D. J. Klionsky, M. Ohsumi, and Y. Ohsumi. 1998. A protein conjugation system essential for autophagy. *Nature* **395**:395–398.
 39. Ohsumi, Y. 2001. Molecular dissection of autophagy: two ubiquitin-like systems. *Nat. Rev. Mol. Cell Biol.* **2**:211–216.
 40. Pedersen, K. W., Y. van der Meer, N. Roos, and E. J. Snijder. 1999. Open reading frame 1a-encoded subunits of the arterivirus replicase induce endoplasmic reticulum-derived double-membrane vesicles which carry the viral replication complex. *J. Virol.* **73**:2016–2026.
 41. Peiris, J. S., Y. Guan, and K. Y. Yuen. 2004. Severe acute respiratory syndrome. *Nat. Med.* **10**:S88–97.
 42. Peiris, J. S., K. Y. Yuen, A. D. Osterhaus, and K. Stohr. 2003. The severe acute respiratory syndrome. *N. Engl. J. Med.* **349**:2431–2441.
 43. Prentice, E., W. G. Jerome, T. Yoshimori, N. Mizushima, and M. R. Denison. 2004. Coronavirus replication complex formation utilizes components of cellular autophagy. *J. Biol. Chem.* **279**:10136–10141.
 44. Ritchie, K. J., C. S. Hahn, K. I. Kim, M. Yan, D. Rosario, L. Li, J. C. de la Torre, and D. E. Zhang. 2004. Role of ISG15 protease UBP43 (USP18) in innate immunity to viral infection. *Nat. Med.* **10**:1374–1378.
 45. Schlegel, A., T. H. Giddings, Jr., M. S. Ladinsky, and K. Kirkegaard. 1996. Cellular origin and ultrastructure of membranes induced during poliovirus infection. *J. Virol.* **70**:6576–6588.
 46. Schwartz, D. C., and M. Hochstrasser. 2003. A superfamily of protein tags: ubiquitin, SUMO and related modifiers. *Trends Biochem. Sci.* **28**:321–328.
 47. Seto, W. H., D. Tsang, R. W. Yung, T. Y. Ching, T. K. Ng, M. Ho, L. M. Ho, and J. S. Peiris. 2003. Effectiveness of precautions against droplets and contact in prevention of nosocomial transmission of severe acute respiratory syndrome (SARS). *Lancet* **361**:1519–1520.
 48. Shintani, T., and D. J. Klionsky. 2004. Autophagy in health and disease: a double-edged sword. *Science* **306**:990–995.
 49. Spiegel, M., A. Pichlmair, L. Martinez-Sobrido, J. Cros, A. Garcia-Sastre, O. Haller, and F. Weber. 2005. Inhibition of beta interferon induction by severe acute respiratory syndrome coronavirus suggests a two-step model for activation of interferon regulatory factor 3. *J. Virol.* **79**:2079–2086.
 50. Stadler, K., V. Masignani, M. Eickmann, S. Becker, S. Abrignani, H. D. Klenk, and R. Rappuoli. 2003. SARS—beginning to understand a new virus. *Nat. Microbiol.* **1**:209–218.
 51. Storer, A. C., and R. Menard. 1994. Catalytic mechanism in papain family of cysteine peptidases. *Methods Enzymol.* **244**:486–500.
 52. Suhy, D. A., T. H. Giddings, Jr., and K. Kirkegaard. 2000. Remodeling the endoplasmic reticulum by poliovirus infection and by individual viral proteins: an autophagy-like origin for virus-induced vesicles. *J. Virol.* **74**:8953–8965.
 53. Sulea, T., H. A. Lindner, E. O. Purisima, and R. Menard. 2005. Deubiquitination, a new function of the severe acute respiratory syndrome coronavirus papain-like protease? *J. Virol.* **79**:4550–4551.
 54. Thiel, V., K. A. Ivanov, A. Putics, T. Hertzog, B. Schelle, S. Bayer, B. Weissbrich, E. J. Snijder, H. Rabenau, H. W. Doerr, A. E. Gorbalenya, and J. Ziebuhr. 2003. Mechanisms and enzymes involved in SARS coronavirus genome expression. *J. Gen. Virol.* **84**:2305–2315.
 55. van der Hoek, L., K. Pyrc, M. F. Jebbink, W. Vermeulen-Oost, R. J. Berkhout, K. C. Wolthers, P. M. Wertheim-van Dillen, J. Kaandorp, J. Spaargaren, and B. Berkhout. 2004. Identification of a new human coronavirus. *Nat. Med.* **10**:368–373.
 56. Wilkinson, K. D. 2000. Ubiquitination and deubiquitination: targeting of proteins for degradation by the proteasome. *Semin. Cell Dev. Biol.* **11**:141–148.
 57. Wong, T. W., C. K. Lee, W. Tam, J. T. Lau, T. S. Yu, S. F. Lui, P. K. Chan, Y. Li, J. S. Breese, J. J. Sung, and U. D. Parashar. 2004. Cluster of SARS among medical students exposed to single patient, Hong Kong. *Emerg. Infect. Dis.* **10**:269–276.
 58. Woo, P. C., S. K. Lau, C. M. Chu, K. H. Chan, H. W. Tsoi, Y. Huang, B. H. Wong, R. W. Poon, J. J. Cai, W. K. Luk, L. L. Poon, S. S. Wong, Y. Guan, J. S. Peiris, and K. Y. Yuen. 2005. Characterization and complete genome sequence of a novel coronavirus, coronavirus HKU1, from patients with pneumonia. *J. Virol.* **79**:884–895.
 59. Wu, C. Y., J. T. Jan, S. H. Ma, C. J. Kuo, H. F. Juan, Y. S. Cheng, H. H. Hsu, H. C. Huang, D. Wu, A. Brik, F. S. Liang, R. S. Liu, J. M. Fang, S. T. Chen, P. H. Liang, and C. H. Wong. 2004. Small molecules targeting severe acute respiratory syndrome human coronavirus. *Proc. Natl. Acad. Sci. USA* **101**:10012–10017.
 60. Yang, H., M. Yang, Y. Ding, Y. Liu, Z. Lou, Z. Zhou, L. Sun, L. Mo, S. Ye, H. Pang, G. F. Gao, K. Anand, M. Bartlam, R. Hilgenfeld, and Z. Rao. 2003. The crystal structures of severe acute respiratory syndrome virus main protease and its complex with an inhibitor. *Proc. Natl. Acad. Sci. USA* **100**:13190–13195.
 61. Yu, I. T., Y. Li, T. W. Wong, W. Tam, A. T. Chan, J. H. Lee, D. Y. Leung, and T. Ho. 2004. Evidence of airborne transmission of the severe acute respiratory syndrome virus. *N. Engl. J. Med.* **350**:1731–1739.
 62. Yuan, W., and R. M. Krug. 2001. Influenza B virus NS1 protein inhibits conjugation of the interferon (IFN)-induced ubiquitin-like ISG15 protein. *EMBO J.* **20**:362–371.
 63. Ziebuhr, J. 2005. The coronavirus replicase. *Curr. Top. Microbiol. Immunol.* **287**:57–94.